Pergamon

*Acta mater.* Vol. 46, No. 12, pp. 4153–4159, 1998

Printed in Great Britain
PII: S1359-6454(98)00119-0
1359-6454/98 $19.00 + 0.00

# STEADY-STATE CREEP IN AN INCLUSION BEARING MATERIAL BY PLASTIC ACCOMMODATION

**E. SATO[1]†, T. OOKAWARA[2], K. KURIBAYASHI[1] and S. KODAMA[2]**

[1]The Institute of Space and Astronautical Science, 3-1-1 Yoshinodai, Sagamihara 229, Japan and
[2]Shonan Institute of Technology, 1-1-25 Nishikaigan, Tujido, Fujisawa 251, Japan

*(Received 7 October 1997; accepted 17 March 1998)*

**Abstract**—The stress relaxation in an inclusion bearing material at high temperatures under an external load has been examined. Independently from the analysis by Mori *et al.* (*Acta mater.*, 1997, **45**, 429), it has been ascertained that the material reveals steady-state creep even with only matrix plastic flow (multiaxial power-law creep) operating, through both variational principles analysis and finite element method (FEM). The characteristic of nonuniform stress distribution, which brings about steady-state creep, has been discussed. The dependence of the steady-state creep rate on inclusion aspect ratio and volume fraction has been also obtained through FEM analysis. © *1998 Acta Metallurgica Inc. Published by Elsevier Science Ltd. All rights reserved.*

## 1. INTRODUCTION

The following papers, which deal with stress relaxation by matrix plastic flow in an inclusion bearing material at high temperatures, have attracted the attention of the present authors. Those by Mori *et al.* [1, 2] studied stress relaxation by several mechanisms under an external load using variational principles analysis, and have concluded that an inclusion bearing material eventually stops creep as the matrix approaches a uniform hydrostatic state if other relaxation mechanisms than matrix plastic flow, such as interfacial sliding, diffusion and debonding, do not operate. They also performed a calculation of finite element method (FEM) and ascertained the eventual stop of creep.

Since discontinuous fiber reinforced metal matrix composites (MMCs) are considered to be a strong candidate for high temperature materials of relatively low cost, it would be appreciated if MMCs would show high creep resistance through preventing other interfacial relaxation mechanisms than matrix plastic flow. In contrast to the above conclusion, there have been several studies which have treated steady-state creep of MMCs only with matrix plastic flow.‡ These can be classified into three categories: approximate analyses known as the shear-lag model [3–7], analyses using a self- consistent differential method [8–11] and numerical analyses using FEM [12, 13].

The shear-lag model states that due to the presence of the fibers, the shearing rate of the matrix and thus the external load should be increased to maintain the same creep rate. The self-consistent differential method calculates the stiffness of a material consisting of a power-law elastic matrix and a rigid inclusion, which corresponds to the steady-state creep rate. FEM calculates the matrix flow which obeys a multiaxial power-law based on the $J_2$-flow theory in a material consisting of a matrix and an inclusion. Among these, the shear-lag model is not self-consistent in terms of stress, but the other two are self-consistent, and the discrepancy with the analysis based on variational principles and FEM by Mori *et al.* [1, 2] is very puzzling.

The aim of the present paper is to reexamine the analysis of Mori *et al.* Using both variational principles and FEM to ascertain the existence of steady-state creep in MMCs with only matrix plastic flow operating. The characteristic of creep deformation with nonuniform stress distribution, which brings about steady-state creep, is discussed. The obtained steady-state creep rates are compared with the results of the self-consistent analysis.

## 2. ANALYTICAL

The problem is first treated analytically. Consider that an external stress $\sigma_{ij}^{A}$ is applied on a composite **D** containing an inclusion **Ω** surrounded by a matrix **M**. Let the body be isotropic and elastically uniform, for simplicity. The matrix only creeps without threshold stress, and interfacial mechanisms, such as sliding, diffusion and debonding, do not occur. Suppose a plastic strain $\varepsilon_{ij}^{*}$ *which is not necessarily uniform*, is introduced *in* **M**, *not in* **Ω**, to relax $\sigma_{ij}^{A}$, and it generates a displacement $u_i$ and an internal stress $\sigma_{ij}$. The summation convention is employed throughout this paper.

†To whom all correspondence should be addressed.

‡Studies of MMCs on room temperature deformation or on creep with one of the interfacial mechanisms other than matrix plastic flow are not referred to.

In Section 2.1, the above problem is analyzed through variational principles to prove the existence of steady-state creep. The concrete strain rate distribution during steady-state creep is given in Section 2.2 for the case of the Newtonian viscous matrix. In Section 2.3, the obtained creep behavior is discussed.

### *2.1. Analysis based on variational principles*

Mori *et al.* [1, 2] concluded that complete relaxation occurs when the total stress in the matrix becomes hydrostatic, as follows. They first calculated the total energy change $F$ due to $\varepsilon_{ij}^{*}$

$$F = \tfrac{1}{2}\int_D \sigma_{ij}(u_{i,j} - \varepsilon_{ij}^{*})\,\mathrm{d}\mathbf{v} - \int_D \sigma_{ij}^{\mathrm{A}}\varepsilon_{ij}^{*}\,\mathrm{d}\mathbf{v}$$
$$= -\int_M (\tfrac{1}{2}\sigma_{ij} + \sigma_{ij}^{\mathrm{A}})\varepsilon_{ij}^{*}\,\mathrm{d}\mathbf{v}. \qquad (1)$$

Here

$$\int_D \sigma_{ij}u_{i,j}\,\mathrm{d}v = 0$$

and $\varepsilon_{ij}^{*} = 0$ in $\Omega$ are used. Next, they applied Lagrange's undetermined multiplier method to obtain the energy minimum state by $\varepsilon_{ij}^{*}$ which satisfies $\varepsilon_{ii}^{*} = 0$. Since the variation of

$$\bar{F} = F + \int_M \lambda\varepsilon_{ii}^{*}\,\mathrm{d}\mathbf{v}$$

is given by

$$\delta\bar{F} = \int_M (\sigma_{ij} + \sigma_{ij}^{\mathrm{A}} - \lambda\delta_{ij})\delta\varepsilon_{ij}^{*}\,\mathrm{d}\mathbf{v} + \left(\int_M \varepsilon_{ii}^{*}\,\mathrm{d}\mathbf{v}\right)\delta\lambda, \quad (2)$$

they concluded that the energy minimum state is achieved, when $\sigma_{ij}$ satisfies

$$\sigma_{ij} + \sigma_{ij}^{\mathrm{A}} = \lambda\delta_{ij} \text{ and } \lambda = \text{constant in } \mathbf{M}. \qquad (3)$$

This implies that complete relaxation occurs when the total stress in the matrix becomes hydrostatic.

It is important to note that the above conclusion by Mori *et al.* is correct, however it *does not mention the existence of* $\sigma_{ij}$*, which satisfies equation (3).*

On the contrary, in the following analysis it will be shown that $\bar{F}$ cannot reach a minimum for the special strain $\varepsilon_{ij}^{*}$ and the creep of the composite continues eternally in the case of the Newtonian viscous matrix. This $\varepsilon_{ij}^{*}$ is given as a hypothetical elastic strain in $\mathbf{M}$ caused by $\sigma_{ij}^{\mathrm{A}}$ in the composite consisting of an elastic $\mathbf{M}$ with Poisson ratio 0.5 and a rigid $\Omega$. $\varepsilon_{ij}^{*}$ can be regarded as plastic (creep) strain in $\mathbf{M}$ because $\varepsilon_{ij}^{*} = 0$ in $\Omega$ and $\varepsilon_{ii}^{*} = 0$ in $\mathbf{M}$. In addition, it does not generate any additional internal stress because it satisfies the compatibility condition [14]. Since the stress state in the composite after the generation of $\varepsilon_{ij}^{*}$ is identical to that before the generation, the generation of $\varepsilon_{ij}^{*}$ can repeat eternally and thus steady-state creep appears. During this steady-state creep, the total energy

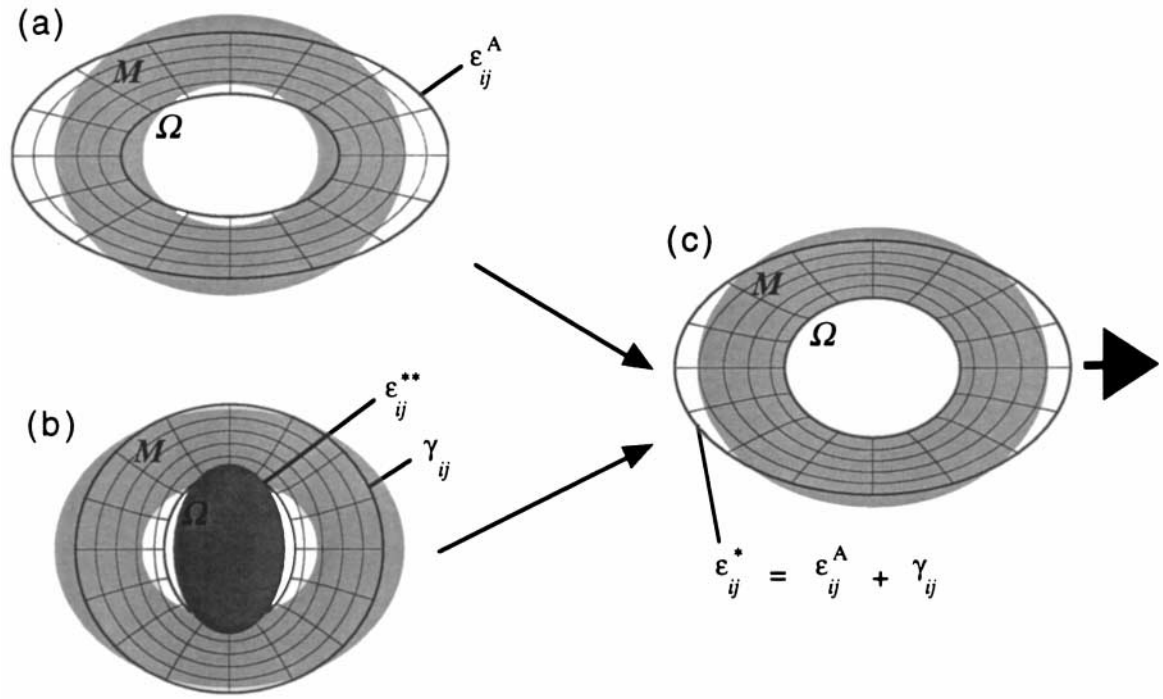


Fig. 1. Schematic of the steady-state creep of MMC with a Newtonian viscous matrix. (a) Uniform plastic strain $\varepsilon_{ij}^{\mathrm{A}}$ caused by $\sigma_{ij}^{\mathrm{A}}$ assuming that $\Omega$ does not exist. (b) Total strain $\gamma_{ij}$ caused by the hypothetical eigenstrain $\varepsilon_{ij}^{**}$ in $\Omega$; $\varepsilon_{ij}^{**}$ is defined so as to give a constant value of $-\varepsilon_{ij}^{\mathrm{A}}$ to $\gamma_{ij}$ in $\Omega$. (c) $\varepsilon_{ij}^{*}$ is given through superimposing $\varepsilon_{ij}^{\mathrm{A}}$ and $\gamma_{ij}$. It can be regarded as plastic strain in $\mathbf{M}$, and generates no additional internal stress.

change cannot reach a minimum because equation (3) is never satisfied.

### 2.2. Calculation of steady-state creep rate for Newtonian viscous matrix

The special matrix strain $\varepsilon_{ij}^{*}$ which decreases the total energy change infinitely for a composite with a Newtonian viscous matrix, is given through superimposing two hypothetical strains, as shown in Fig. 1: (a) one is a uniform plastic strain $\varepsilon_{ij}^{A}$ caused by $\sigma_{ij}^{A}$ in the case where $\Omega$ does not exist, and (b) another is a total strain $\gamma_{ij}$, which is caused by the hypothetical eigenstrain $\varepsilon_{ij}^{**}$ in $\Omega$; $\varepsilon_{ij}^{**}$ is defined so as to give a constant value of $-\varepsilon_{ij}^{A}$ to $\gamma_{ij}$ in $\Omega$. Next, (c) consider $\varepsilon_{ij}^{*}=\varepsilon_{ij}^{A}+\gamma_{ij}$ as the only eigenstrain in **D**. This $\varepsilon_{ij}^{*}$ can be regarded as plastic strain in **M** because $\varepsilon_{ij}^{*}=0$ in $\Omega$ and $\varepsilon_{ii}^{*}=0$ in **M**. In addition, it does not generate any additional internal stress in **D** because it satisfies the compatibility condition [14].

For the case of an ellipsoidal inclusion, $\gamma_{ij}$ in $\Omega$ is given as

$$\gamma_{ij}^{\infty}(\Omega)=-S_{ijkl}\varepsilon_{kl}^{**}, \text{ for an infinite matrix} \tag{4a}$$

and

$$\gamma_{ij}(\Omega)=(1-f\ )\gamma_{ij}^{\infty}(\Omega)+f\varepsilon_{ij}^{**}, \text{ for a finite matrix} \tag{4b}$$

where $S_{ijkl}$ is Eshelby's tensor [15, 16], and $f$ is the volume fraction of $\Omega$. To obtain equation (4b), the image stress is approximated to be uniform, and Tanaka–Mori theorem [17] is used. From the restriction that $\gamma_{ij}$ in $\Omega$ is constant with a value of $-\varepsilon_{ij}^{A}$, $\varepsilon_{ij}^{**}$ is given as

$$\varepsilon_{ij}^{**}=-((1-f)S_{klij}+fI_{klij})^{-1}\varepsilon_{kl}^{A}. \tag{5}$$

The average of $\varepsilon_{ij}^{*}=\varepsilon_{ij}^{A}+\gamma_{ij}$ in the composite of volume $V_D$ is calculated as

$$\begin{aligned}\bar{\varepsilon}_{ij}&=\frac{1}{V_D}\int_D \varepsilon_{ij}^{*}\,\mathrm{d}\mathbf{v}=\varepsilon_{ij}^{A}+f\varepsilon_{ij}^{**}\\&=\left(I_{ijkl}-\left(\frac{1-f}{f}S_{klij}+I_{klij}\right)^{-1}\right)\varepsilon_{kl}^{A}.\end{aligned} \tag{6}$$

Here

$$\int_D \gamma_{ij}\,\mathrm{d}\mathbf{v}=\int_\Omega \varepsilon_{ij}^{**}\,\mathrm{d}\mathbf{v}=f\varepsilon_{ij}^{**}$$

is used. The total energy change due to $\varepsilon_{ij}^{*}$ can be easily calculated from equation (1), since it generates no additional stress, i.e. $\sigma_{ij}=0$ in equation (1),

$$\begin{aligned}F&=-\int_D \sigma_{ij}^{A}\varepsilon_{ij}^{*}\,\mathrm{d}\mathbf{v}\\&=-V_D\sigma_{ij}^{A}\left(I_{ijkl}-\left(\frac{1-f}{f}S_{klij}+I_{klij}\right)^{-1}\right)\varepsilon_{kl}^{A}.\end{aligned} \tag{7}$$

Equation (7) implies that the total energy change decreases infinitely and never reaches a minimum with increasing $\varepsilon_{ij}^{A}$.

For analyzing steady-state creep, each strain quantity should be re-identified as a strain rate quantity.

In the case of axial symmetry, i.e. uniaxially loaded material with a spheroidal inclusion whose major axis is parallel to the loading axis, equation (4a) can be rewritten using only the (1,1) component,

$$\dot{\gamma}_{11}^{\infty}(\Omega)=S^{*}\dot{\varepsilon}_{11}^{**} \tag{8}$$

$$S^{*}=\frac{-9a^2}{2(a^2-1)^2}+\frac{3a(a^2+\frac{1}{2})}{(a^2-1)^{5/2}}\cosh^{-1}a,$$

for a prolate spheroid (9a)

$$S^{*}=\frac{-9a^2}{2(1-a^2)^2}+\frac{3a(a^2+\frac{1}{2})}{(1-a^2)^{5/2}}\cos^{-1}a,$$

for an oblate spheroid (9b)

and

$$S^{*}=\tfrac{2}{5} \text{ for a sphere,} \tag{9c}$$

where $a$ is the inclusion aspect ratio. The tensile creep rate of the body is then given by

$$\bar{\dot{\varepsilon}}_{11}=\frac{1-f}{1-f+f/S^{*}}\dot{\varepsilon}_{11}^{A} \tag{10}$$

where $\dot{\varepsilon}_{11}^{A}$ is the tensile creep rate of the matrix alone under the same tensile load. Equation (10) is the specific form of equation (6).

### 2.3. Behavior of steady-state creep rate for Newtonian viscous matrix

For a composite with a Newtonian viscous matrix, the steady-state creep rates normalized by the creep rate of the matrix alone, $\bar{\dot{\varepsilon}}_{11}/\dot{\varepsilon}_{11}^{A}$, are calculated using equation (10) and plotted against the aspect ratio, $a$, in Fig. 2 by solid lines. This figure also shows the creep rates calculated by Lee and Mear (equation (16) of Ref. [10]) by broken lines.

Both calculations show a similar behavior: the creep rate decreases with increasing $a$ beyond $a$ greater than one. It increases with decreasing $a$ for $a$ less than one, shows a maximum at $a=2/3$, and then decreases with a further decrease in $a$. For a fixed value of $a$, it decreases with increasing $f$.

It should be noted that the behavior with $a\to 0$ is contrary to the simple rule of mixture. The error in the rule of mixture results from the three-dimensional constraint: since the components of the matrix creep rate perpendicular to the tensile axis, $\dot{\varepsilon}_{22}^{*}$ and $\dot{\varepsilon}_{33}^{*}$, should be zero in the limit of $a\to 0$, the tensile component, $\dot{\varepsilon}_{11}^{*}$, should also be zero.

The calculation by Lee and Mear [10] always shows a smaller creep rate than the present values. This is caused by the tricky procedure of treating

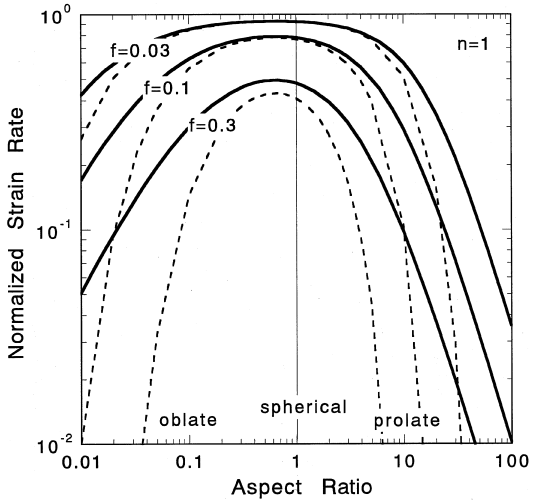


Fig. 2. Dependence of the creep rate on the inclusion aspect ratio with matrix stress exponent $n = 1$. The creep rate is normalized by the matrix creep rate. The solid lines are for this study (equation (10)), and the broken lines are for the analysis of Lee and Mear (equation (16) of Ref. [10]).

the image stress in their calculation: equation (15) in Ref. [10]. On the other hand, the Tanaka–Mori theorem [17] was used for calculating the image stress in equation (4b). This problem is again discussed in a comparison with FEM analysis in Section 3.1.

## 3. FINITE ELEMENT METHOD

The statement in Section 2.1, which states that the analysis of Mori *et al.* [1, 2] does not mention the existence of $\sigma_{ij}$ which satisfies equation (3), is valid for any creeping matrix, and the specific tensile creep rate of the material, $\bar{\dot{\varepsilon}}_{11}$, has been calculated in Section 2.2 for the Newtonian viscous matrix. However it is required to calculate $\bar{\dot{\varepsilon}}_{11}$ for a metallic matrix, which obeys a multiaxial power-law based on $J_2$-theory. FEM analysis is one of the methods of the calculation, though Mori *et al.* [1, 2] reported the eventual stop of creep in a two-dimensional FEM analysis.

In Section 3.1, the steady-state creep in a two-dimensional analysis is shown and the error in the analysis of Mori *et al.* is pointed out. In Section 3.2, creep behavior of MMCs in three dimensions is calculated and the dependence of the creep rate on inclusion aspect ratio is discussed. The actual FEM calculations were carried out using MARC K6.2, a general purpose FEM code for structural analysis.

### *3.1. Plane strain problem*

A continuous fiber reinforced metal matrix composite is subjected to an applied tensile stress perpendicular to the fiber. The model, shown in Fig. 3, contains a quarter of an elastic cylindrical fiber and surrounding rectangular matrix which creeps according to a multiaxial power-law based on $J_2$-

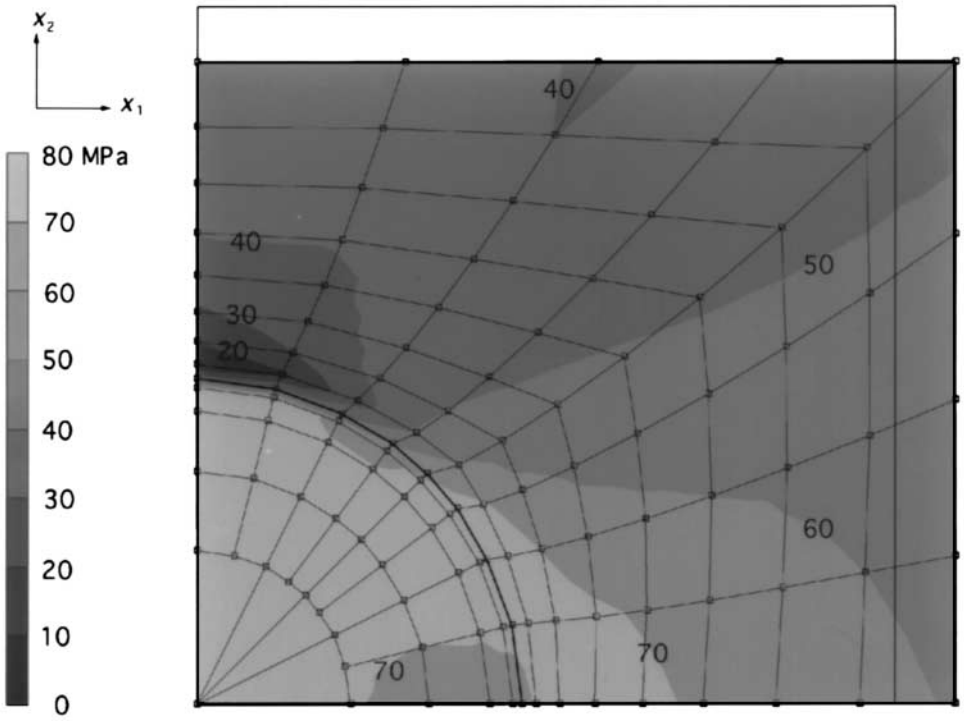


Fig. 3. Two-dimensional FEM analysis showing the stress distribution of tensile component $\sigma_{11}$ in the steady state creep of $\varepsilon = 0.08$. A composite, consisting of an elastic cylindrical fiber of $f = 0.17$ and a surrounding matrix which creeps with stress exponent $n = 3$, is subjected to an applied tensile stress in the $x_1$-direction. The constant dilatation option is used in the calculation.

theory:

$$\dot{\varepsilon}_{ij} = \tfrac{3}{2} B(\tfrac{3}{2}\sigma_{kl}'\sigma_{kl}')^{(n-1)/2}\sigma_{ij}' \qquad (11)$$

where $\sigma_{ij}'$ are the deviatoric components of $\sigma_{ij}$ and $B$ is a constant. The materials constants are as follows: fiber volume fraction $f$ is 0.17, matrix stress exponent $n$ is 3, $B$ in equation (11) is $8 \times 10^{-10}$ $\mathrm{MPa}^{-3}\,\mathrm{s}^{-1}$, Young's modulus of both the matrix and the inclusion is 200 GPa and the Poisson ratio of both is 0.33. The right-hand side of the model is subjected to a constant tensile load in the $x_1$-direction which corresponds to an initial stress of 50 MPa. The periodic boundary condition is adopted, i.e. the top and the right sides of the model remain straight so that the model remains rectangular in shape.

The model is composed of 100 elements, 64 for the matrix and 36 for the inclusion, which are four-noded, quadrilateral, isoparametric and plane strain. A Newton–Raphson technique with adaptive time stepping is used to solve the nonlinear equations associated with creep. Large displacement option, updated Lagrange procedure and finite strain plasticity option are adopted for calculating large creep deformation. In addition, the calculations are performed with a constant dilatation option.

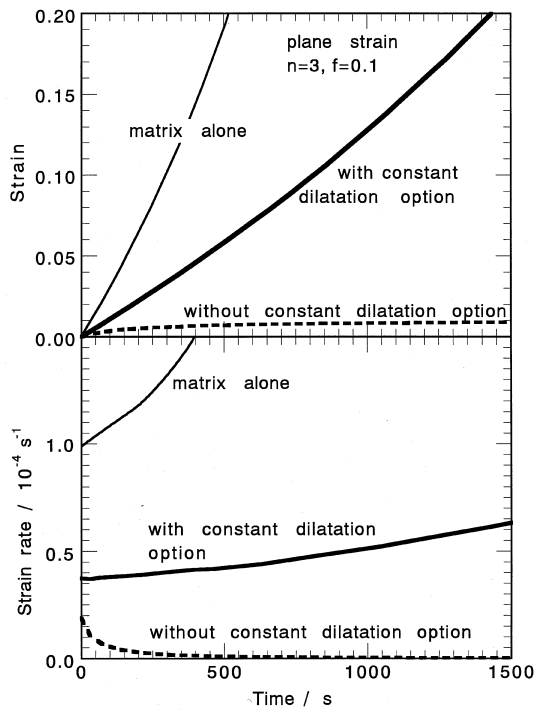


Fig. 4. The creep curves calculated in a two-dimensional FEM analysis. A composite, consisting of an elastic cylindrical fiber of $f = 0.17$ and a surrounding matrix which creeps with stress exponent $n = 3$, is subjected to an applied tensile stress. The calculations are performed with and without the constant dilatation option.

The thick solid line in Fig. 4 shows the creep curve of the composite and the thin solid line shows that of the matrix alone. It is obvious that the composite keeps creeping continuously with a lower creep rate than the matrix. The creep rate of the composite decreases slightly during the first 30 s, in which period the steady-state stress distribution is achieved, and then increases with decreasing the cross section of the composite under a constant load. The steady-state stress distribution of the tensile component, $\sigma_{11}$, at $\varepsilon = 0.08$ is shown in Fig. 3. The inclusion supports larger stress (60–80 MPa) than the applied stress (46 MPa), and the strain is concentrated in the part of the matrix adjacent to the inclusion.

On the other hand, the calculation by Mori *et al.* [1, 2] has been performed without the constant dilatation option [18], which is necessary to avoid locking of elements with large, nearly incompressive strains [19]. The calculation was performed using the above model, but without the constant dilatation option. The obtained creep curves are shown in Fig. 4 by broken lines, which show the false behavior of the eventual stop of the creep quite similar to Fig. 2 of Ref. [2]. The obtained stress distribution, where the equivalent stress (von Mises stress) becomes almost zero in the matrix, is also similar to Fig. 2 of Ref. [1]. However, it is found that the components of the stress such as $\sigma_{11}$, $\sigma_{22}$ and $\sigma_{33}$ are non-zero and non-constant in the matrix; this indicates that the calculated stress state is false because it does not satisfy the equilibrium condition.

### *3.2. Axial symmetry problem*

Creep behavior of three-dimensional, discontinuous fiber reinforced MMC is calculated. The model contains a quarter of an elastic spheroidal fiber and a surrounding cylindrical matrix which creeps according to multiaxial power-law of equation (11). The materials constants are as follows: fiber volume fraction $f$ is 0.068, matrix stress exponent $n$ is 1 and 3, $B$ in equation (11) is $1 \times 10^{-2}$ $\mathrm{MPa}^{-3}\,\mathrm{s}^{-1}$ and $1 \times 10^{-6}$ $\mathrm{MPa}^{-3}\,\mathrm{s}^{-1}$, Young's moduli of the matrix and the inclusion are 30 and 120 GPa, respectively, and Poisson ratio of both is 0.34. Several composites with different inclusion aspect ratios are calculated and the aspect ratio of the matrix is set to be equal to that of the inclusion.

Meshing of the model is the same as in the case of the plane strain problem (Fig. 3), although the elements are four-noded, quadrilateral, isoparametric and axially symmetric with the symmetry axis being the bottom line of the model ($x_1$-direction). An axial tensile load ($x_1$-direction) corresponding to an initial stress of 100 MPa is applied. A Newton–Raphson technique with adaptive time stepping, large displacement, updated Lagrange procedure, finite strain plasticity and constant dilatation options are adopted.

Two boundary conditions are adopted: the first is a free boundary condition which places no restriction on the right and top sides of the model. The second is a pseudo-periodic boundary condition which keeps the top and right sides of the model straight so that the model remains cylindrical in shape. The analytical calculation in Section 2 is based on the former boundary condition for a composite of spheroid shape. The latter boundary condition represents a composite with fibers perfectly aligned in a periodic array. The real composites may have a boundary condition between these two.

Figure 5 shows the calculated dependence of the steady-state creep rate on the inclusion aspect ratio with matrix stress exponent $n = 1$ and 3. The creep rate is normalized by the matrix creep rate. Circles indicate the free boundary condition and squares indicate the pseudo-periodic boundary condition. The analytical calculations performed in this study (equation (10)) for $n = 1$ and those by Lee and Mear (equation (16) of Ref. [10]) with $n = 1$ and 3 are also shown by the thin solid, broken and chain lines, respectively.

The two FEM calculations show that the creep rate decreases with both increasing aspect ratio and stress exponent. This implies that the strengthening effect of fibers is stronger with both higher aspect ratio and stress exponent. In addition, it is obvious that the pseudo-periodic boundary condition results in a lower creep rate than the free boundary condition. Comparing the calculations for the free boundary condition, the analytical calculation of this study shows a better agreement with the FEM analysis than that by Lee and Mear. This proves the correctness of the procedure of treating image stress used in this study, which was already discussed in Section 2.3. However, the analytical result of this study shows a little larger value than FEM. This is due to the difference in the shape of the matrix; the cylindrical matrix in FEM has a larger portion of a further part from the inclusion than the spheroidal matrix in the analytical study.

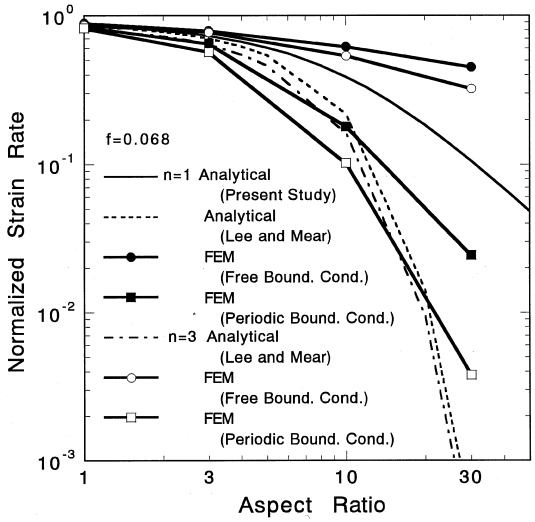


Fig. 5. Dependence of the creep rate on the inclusion aspect ratio with matrix stress exponents of $n = 1$ and 3 and inclusion volume fraction $f = 0.068$. The creep rate is normalized by the matrix creep rate. The circles are for FEM analysis with the free boundary condition, and the squares are for the FEM analysis with the pseudo-periodic boundary condition. In addition, the analysis of this study (equation (10)) is shown by the thin solid line, and the analysis of Lee and Mear (equation (16) of Ref. [10]) is shown by thin broken and chain lines.

## 4. SUMMARY

The stress relaxation in an inclusion bearing material without other interfacial relaxation mechanisms than matrix plastic flow has been examined, and the existence of steady-state creep has been proved.

1. Although it is true that the energy minimum is achieved when the matrix becomes hydrostatic in stress, the existence of the relaxation strain for the energy minimum state is not proved.
2. For a material with a Newtonian viscous matrix, the special plastic strain, which is given as a hypothetical elastic strain in a body consisting of elastic matrix and a rigid inclusion, generates no additional internal stress and thus steady-state creep appears.
3. Self-consistent analysis calculates a smaller creep rate because of the tricky procedure in treating image stress.
4. For a material consisting of a creeping matrix under a multiaxial power-law and an elastic inclusion, FEM analysis reveals steady-state creep in both two- and three-dimensional analyses. Without the constant dilatation option, a false result indicating eventual stop of creep is obtained.
5. The dependence of the steady-state creep rate on inclusion aspect ratio and volume fraction is obtained through FEM analysis.

*Acknowledgements*—Critical discussion with T. Mori, Cambridge University, and a private communication [18] including the MARC input file used in Ref. [1, 2] from Y. Nakasone, Science University of Tokyo are appreciated.

## REFERENCES

1. Mori, T., Huang, J. H. and Taya, M., *Acta mater.*, 1997, **45**, 429.
2. Mori, T., Tanaka, K., Nakasone, Y., Huang, J. and Taya, M., *Key Engng Mater.*, 1997, **127-131**, 1145.
3. Kelly, A. and Street, K. N., *Proc. R. Soc. Lond.*, 1972, **A328**, 283.
4. McLean, D., *J. Mater. Sci.*, 1972, **7**, 98.
5. Lilholt, H., *Comp. Sci. Technol.*, 1985, **22**, 277.
6. Goto, S. and McLean, M., *Acta metall. mater.*, 1991, **39**, 165.

7. McMeeking, R. M., *Int. J. Solids Struct.*, 1993, **30**, 1807.
8. Duva, J. M., *J. Engng Mater. Technol.*, 1984, **106**, 317.
9. Duva, J. M. and Storm, D., *J. Engng Mater. Technol.*, 1989, **111**, 368.
10. Lee, B. L. and Mear, M. E., *J. Mech. Phys. Solids*, 1991, **39**, 627.
11. Willis, J. R., *Mater. Sci. Engng*, 1994, **A175**, 7.
12. Dragone, T. L. and Nix, W. D., *Acta metall.*, 1990, **38**, 1441.
13. Kim, K. T. and McMeeking, R. M., *Mech. Mater.*, 1995, **20**, 153.
14. Reissner, H., *Z. Angew. Math. Mech.*, 1931, **11**, 1.
15. Eshelby, J. D., *Proc. R. Soc.*, 1957, **A241**, 376.
16. Eshelby, J. D., *Proc. R. Soc.*, 1959, **A252**, 561.
17. Tanaka, K. and Mori, T., *J. Elasticity*, 1972, **2**, 199.
18. Nakasone, Y., private communication.
19. Nagtegaal, J. C., Parks, D. M. and Rice, J. R., *Computer Meth. Appl. Mech. Engng*, 1974, **4**, 153.